

EVALUATING HIGH-TEMPERATURE CORROSION OF SiC REFRACTORIES BY COAL SLAG USING IMPROVED EXPERIMENTAL METHOD

Shixian Zhao, Hongxia Li, Binli Cai, Honggang Sun, Gang Wang

Sinosteel Luoyang Institute of Refractories Research Co., Ltd., Luoyang, China

ABSTRACT

SiC refractories are currently utilized as lining materials for water-cooled gasifier at a service temperature lower than 1300°C. Very few researches have been reported on the corrosion of SiC materials at even higher temperature. In this paper, corrosion behavior of SSiC and Si₃N₄-SiC refractories interacted with coal slag was investigated at 1500°C under reducing atmosphere using improved rotary slag testing method. Moreover, interactions between refractory materials and molten slag were also predicted by thermodynamic calculations using modified model under the same conditions. The results showed that SSiC and Si₃N₄-SiC refractories presented the similar stability and corrosion behavior under simulated gasification conditions. SiC reacted with FeO to form Si-Fe-C alloy on the surface of the corroded materials. Meanwhile, SiO₂ phase was also formed by oxidation of SiC in the experimental atmosphere and then dissolved into the molten slag eventually.

INTRODUCTION

Coal gasification technology is a process that converts coal or the combustible part of the coal tar at high temperature and pressure into flammable gas mainly composed of carbon monoxide and hydrogen[1]. Coal water slurry gasification technology is one of the most widely used coal gasification technologies. It is typically operated between 1300 and 1600 °C at pressures of 2.0–6.9 MPa under a strongly reducing atmosphere[2,3]. Because of the complex working conditions in the coal gasifier, high chrome refractories are usually adopted as lining materials in the gasifier due to their excellent corrosion resistance. However, Cr⁺⁶ are formed by the reactions of CaO, Na₂O, and K₂O with Cr₂O₃, which is easily soluble in water[4]. As carcinogenic substance, Cr⁺⁶ pollutes the environment and endangers people's health seriously if the residual bricks are not disposed properly[5]. Therefore, research on chrome-free materials as gasifier lining has great significance on environmental protection and occupational health.

SiC is utilized extensively as high-temperature structural material due to its excellent thermal shock stability, high-temperature strength, and low coefficient of thermal expansion[6,7], and it is used as lining material of gasifiers with water-cooled walls because of its excellent thermal conductivity.

However, the working temperature of SiC is lower than 1300°C in coal gasifiers with water-cooled walls. Few researches on the slag corrosion resistance of SiC materials at higher temperatures has been reported so far. In this paper, the dynamic corrosion of SSiC and Si₃N₄ bonded SiC interaction with coal slag has been investigated in an improved rotary drum furnace under simulated gasifier conditions at 1500°C. Moreover, the corrosion process has also been simulated by thermodynamic calculations based on an improved model. Finally, the mechanism of the slag-induced corrosion of SiC samples in a reducing atmosphere has been analyzed based on thermodynamic simulation and experimental results.

EXPERIMENTAL AND CALCULATION

Dynamic erosion experiment

To simulate the gasifier atmosphere for the following corrosion test, an atmosphere calibration experiment was conducted in the rotary drum furnace firstly. A mixture of C₂H₂ and O₂ was used as the fuel gas and the FeO content in the quenched slag was analyzed to determine the atmosphere.

Then the SSiC and Si₃N₄-SiC bricks were lined into the rotary drum furnace according to Fig.1. The furnace was heated up to 1500°C at a rate of about 200°C/h by firing the C₂H₂ and O₂ gases at the flow ratio determined in the above calibration experiment. Coal slag was put into the furnace and kept the furnace temperature at 1500 °C for 2h. For deslagging, the furnace body was immediately inclined to an angle of 90° and the slag was poured into cold water. Subsequently, the furnace body was restored. This whole process was repeated for 20 h to complete the corrosion experiment. After the furnace was cooled down, the obtained corroded samples were collected and cut for further analysis. The polished samples were examined by EDS for morphological observation and compositional analysis.

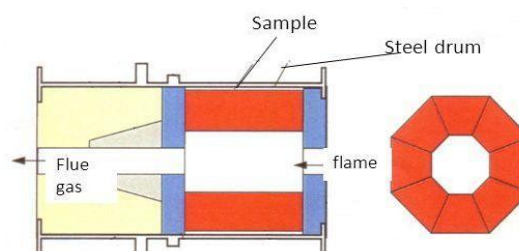


Fig.1: The diagram of the rotary drum furnace

Small quantities of the samples were pulverized and analyzed by XRD to examine the crystalline phases.

Thermodynamic calculations

Thermodynamic calculations were performed using the FactPS and FToxid databases that are comprised in version 6.4 of the FactSage™ software.

We calculated phase composition and gas partial pressures after SiC oxidation process under the atmosphere determined by the calibration experiment. Moreover, we simulated thermodynamic equilibrium phases after the interaction of SiC with slag according to the model illustrated in Fig.2. Therein, the left zone(S) is defined as slag and the right zone(R) as SiC sample, which are correlated according to the equation of (R)+(S)=100g. The percentage of SiC in the mixture is denoted by A ($A=(R)/[(R)+(S)]*100\%$).

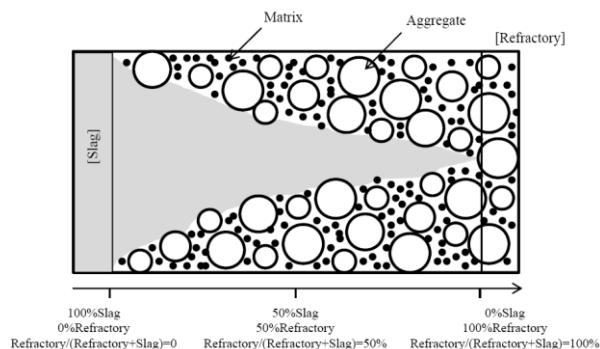


Fig.2: Thermodynamic calculation model

RESULTS AND DISCUSSION

Atmosphere calibration

The results of the atmosphere calibration are listed in Table1, which reveal that the FeO percentage in the Fe oxides increased gradually with the increase of the C_2H_2/O_2 flow ratio. At a flow ratio of $C_2H_2/O_2 = 45/55$, the FeO percentage in the Fe oxides reached 96.15% after a soaking time of 15min and increased slightly to 98.55% after a prolonged soaking time of 1 h. At a flow ratio of $C_2H_2/O_2 = 50/50$, only a slightly larger FeO percentage of 98.76% was detected in the slag after 15min, which suggests that a further increase of the C_2H_2/O_2 flow ratio presumably causes no further increase of the FeO percentage.

At a C_2H_2/O_2 flow ratio of 45/55, only an amorphous phase was detected in the quenched slag by XRD analysis. This indicates that SiC materials can interact with molten amorphous slag under the experimental conditions. Kwong[2] and Font[8] also detected FeO mainly exist as Fe oxide species in amorphous silicate melt in coal gasifiers, which is in good agreement with the above experimental results. Therefore, a C_2H_2/O_2 flow ratio of 45/55, which can be realized in the simulated gasification

atmosphere, was determined as the performing condition for corrosion testing and calculation procedures.

Tab. 1: Results of the atmosphere calibration

C_2H_2/O_2	Soaking time (mins)	Fe_2O_3 (%)	FeO (%)	$FeO/\Sigma(FeO_n)$ (%)
40/60	15	6.54	3.02	31.59
45/55	15	0.35	8.74	96.15
45/55	60	0.13	8.86	98.55
50/50	15	0.11	8.79	98.76

Microstructure and phase analysis of corroded SiC bricks

Fig.3 shows the microstructure and phase analysis results of SSiC sample. It can be seen that small amount of slag and metal particles exist on the surface of corroded brick. The metal particles are detected as the composition of C, Fe and Si by SEM-EDS analysis. About 1mm reaction layer formed by the penetration of slag which led to unclear interfaces between matrix and aggregates. FeO and SiO_2 as the main phases exist in the reaction layer which is also detected by SEM-EDS. The XRD analysis of corroded SSiC brick shows that new phases of SiO_2 and $CaAl_2Si_2O_8$ were formed comparing to the original brick which only contains SiC and Si. The much lower peak intensity of new formed phases indicates a much thinner reaction layer formed on the surface. Moreover, no metal phases are detected by XRD which is due to the loss of formed metal during slag pouring process.

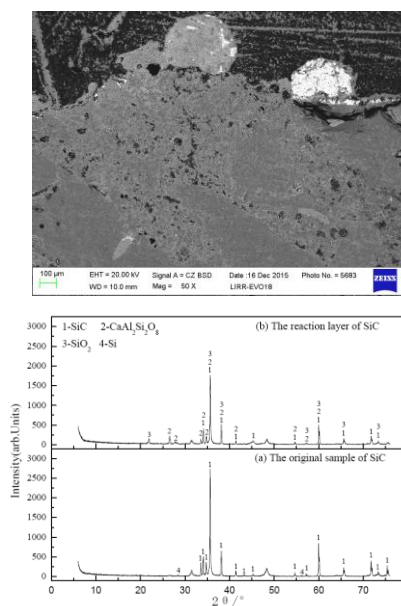


Fig. 3: Microstructure and XRD analysis of corroded SSiC

Fig.4 presents the microstructure and phase analysis results of Si_3N_4 -SiC sample. It can also be seen that small amount of remained slag and metal particles exist on the surface of the

brick. The penetration depth of slag is slightly thinner than that of SSiC. The main phases in the reaction layer are also detected as FeO and SiO₂. The XRD analysis shows that new phase of SiO₂ and Si₂N₂O formed during the corrosion process, which may be caused by oxidation of SiC and Si₃N₄. No CaAl₂Si₂O₈ phase is found in the XRD pattern which is also due to the less slag penetration. Moreover, no metal phases are found either.

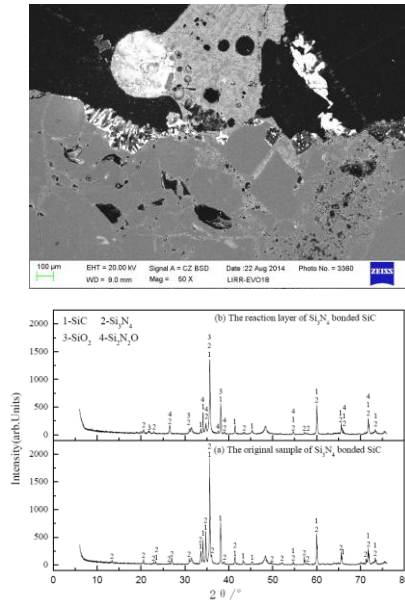


Fig. 4: Microstructure and XRD analysis of corroded Si₃N₄-SiC

Corrosion mechanism-Atmosphere oxidation

In the simulated atmosphere, the O₂ partial pressure is much higher than that SiC and Si₃N₄ could exist stably. Therefore, the SiC and Si₃N₄ will be oxidized to form SiO₂ in the present atmosphere. The calculated phase composition and gas partial pressure after oxidation are shown in Fig. 5. When SiC brick interacted with experimental gases, solid phase of SiO₂ and gas phases of SiO and CO will be formed accordingly. The O₂ partial pressure decreases and then becomes to a table value. However, when the gases interacted with Si₃N₄, both the O₂ and CO partial pressures decrease and become to a table value but the N₂ partial pressure increases accordingly. The solid phases of SiC, SiO₂ and Si₂N₂O and gas phases of SiO, CO, N₂ and NO are formed after oxidation process.

It is well known that SiC and Si₃N₄ will be oxidized when interacted with gases containing O₂ at high temperature. If the O₂ partial pressure is higher, solid SiO₂ layer will be formed on the surface of SiC and Si₃N₄ and inhibit the further oxidation process, which is named passive oxidation. If the O₂ partial pressure is lower, no solid SiO₂ layer exist and the oxidation process will be continued, the process of which is named as active oxidation.

It is reported by Yamaguchi[9] that the critical condition of

passive oxidation and active oxidation of SiC is $P(O_2) = P(SiO + CO)$. When $P(O_2) < P(SiO + CO)$, the active oxidation will proceed. Accordingly, the critical condition of passive oxidation and active oxidation of Si₃N₄ is $P(O_2) = P(SiO + N_2)$. When $P(O_2) < P(SiO + N_2)$, the active oxidation will proceed. It can be seen from Fig. 5 that when the gas-solid reaction between SiC/Si₃N₄ and the gas mixture reached equilibrium state, P(O₂) is lower than P(SiO+CO) and P(SiO+N₂) where the active oxidation proceeded and solid SiO₂ and gases formed accordingly.

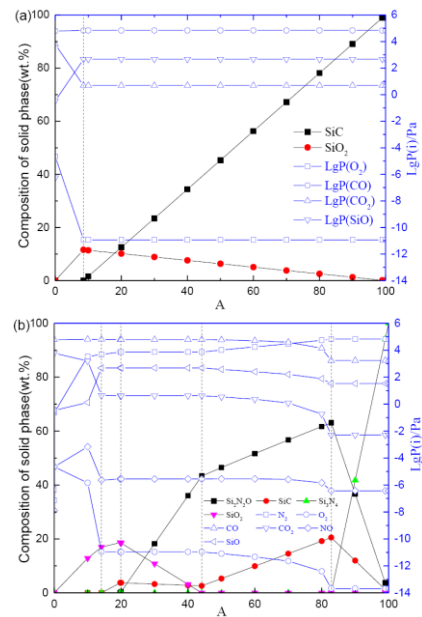


Fig.5: Calculated results of solid phases and gas pressure under simulated atmosphere

Corrosion mechanism-Slag corrosion

In the present experimental atmosphere, the oxidation of SiC and Si₃N₄ will decrease the O₂ partial pressure. The FeO in molten slag will be reduced to Fe which will then reacted with SiC to form FeSi and C. The reaction products of Fe, FeSi, and C interact to form liquid alloys and precipitate into the slag. The largest amount of the liquid alloys was poured into water with the slag, and the remaining liquid alloys adhered to the surface upon cooling.

Fig. 6 shows the calculated results when SiC and Si₃N₄ interacted with molten slag at experimental atmosphere. Solid phase of SiO₂ will be formed when the molten slag interacted with SiC while Si₂N₂O formed when with Si₃N₄. The formed SiO₂ dissolves into the molten slag to cause an increase of SiO₂ content and decrease of CaO and Al₂O₃ in slag.

In the experimental process, the O₂ partial pressure in the furnace was always higher than the O₂ partial pressure when SiC and Si₃N₄ existed stably. Thus, SiC and Si₃N₄ were continuously oxidized and dissolved in the molten slag. Furthermore, the SiO₂

dissolution in the slag became gradually saturated and excessive SiO_2 precipitated on the pore surface, leading to continuous slag penetration. The process comprising dissolution, precipitation of SiO_2 and slag penetration increased the SiO_2 content in the molten slag and the slag viscosity which would weaken further infiltration. Therefore, the molten slag exhibited a much thinner penetration depth into the sample during the present corrosion testing process.

Additionally, SiC could be easily oxidized at present experimental atmosphere but Si_3N_4 will only be oxidized to form $\text{Si}_2\text{N}_2\text{O}$ at relatively lower O_2 partial pressure. Therefore, the molten slag infiltrated deeper in SSiC sample comparing to that in Si_3N_4 -SiC sample.

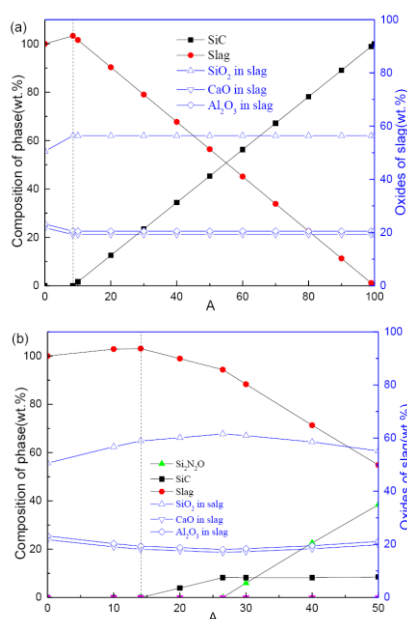


Fig.6: Calculated results of interactions of SiC brick and molten slag

CONCLUSION

In the present experimental atmosphere, the corrosion processes of SSiC and Si_3N_4 -SiC by molten slag are much similar. The solid phase of SiO_2 formed by active oxidation of SiC and Si_3N_4 will dissolve into the molten slag. The oxidation process changed the pore structure on the surface and the molten slag infiltrated into the pores to form a thinner reaction layer.

In the gasification atmosphere, SSiC and Si_3N_4 -SiC bricks will be oxidized by active oxidation process of gases. Moreover, the molten slag could also react with the SiC bricks. Because of the poor wettability of SiC bricks, no remained slag existed on the surface which could not inhibit the active oxidation process and dissolution of SiO_2 . Thus, SSiC and Si_3N_4 -SiC refractories will not be applicable for the water coal slurry gasification.

ACKNOWLEDGMENT

This work was supported by the Foundation and Advanced Technology Research Project of Henan Province, China (162300410043) and National Natural Science Foundation of China (U1604252).

REFERENCES

- [1] He YD. Handbook of modern coal chemical technology. Chemical Industry Press, Beijing; 2004.
- [2] Kwong KS, Petty A, Bennett JP, Krabbe R, Thomas H. Wear Mechanisms of Chromia Refractories in Slagging Gasifiers. *Int J Applied Ceram Tech.* 2007; 4 (6): 503-13.
- [3] Nakano J, Sridhar S, Bennett JP, Kwong KS, Moss T. Interactions of refractory materials with molten gasifier slags, *Int J Hydrogen Energy.* 2011; 36 (7): 4595-604.
- [4] Obana T. Trend of chrome-free refractory materials. *J Tech Association Refract.* 2010; 4(30): 243-9.
- [5] Chen YL, Lai YC, Lin CJ, Chang YK, Ko MS. Controlling sintering atmosphere to reduce the hazardous characteristics of low-energy cement produced with chromium compounds. *J Cleaner Production.* 2013; 43 (5): 45-51.
- [6] Sömiya S, Inomata Y. Silicon Carbide Ceramics-1. Springer Netherlands. 1991; 17(1): 213-38.
- [7] Sömiya S, Mitomo M, Yoshimura M. Silicon Nitride-1. *Concise Encycl Adv Ceram Mater.* 2009; 12(2): 434-7.
- [8] Font O, Querol X, Huggins FE, Chimenos JM, Fernández AI, Burgos S, et al. Speciation of major and selected trace elements in IGCC fly ash. *Fuel.* 2005; 84 (11): 1364-71.
- [9] Yamaguchi A. Practical thermodynamics and its application in high-temperature ceramics. Wuhan Industrial University Press, Wuhan: 1993.

MAILING ADDRESS

andyzhaosx@163.com